scientific reports

Check for updates

OPEN

Green synthesis of 1,5-dideoxy-1,5-imino-ribitol and 1,5-dideoxy-1,5-imino-DL-arabinitol from natural D-sugars over Au/Al_2O_3 and SO_4^{2-}/Al_2O_3 catalysts

Hongjian Gao & Ao Fan✉

A green synthetic route for the synthesis of some potential enzyme active hydroxypiperidine iminosugars including 1,5-dideoxy-1,5-imino-ribitol and 1,5-dideoxy-1,5-imino-DL-arabinitol, starting from commercially available D-ribose and D-lyxose was tested out. Heterogeneous catalysts including Au/Al_2O_3, SO_4^{2-}/Al_2O_3 as well as environmentally friendly reagents were employed into several critical reaction of the route. The synthetic route resulted in good overall yields of 1,5-dideoxy-1,5-imino-ribitol of 54%, 1,5-dideoxy-1,5-imino-D-arabinitol of 48% and 1,5-dideoxy-1,5-imino-L-arabinitol of 46%. The Au/Al_2O_3 catalyst can be easily recovered from the reaction mixture and reused with no loss of activity.

Iminosugars are analogues of carbohydrates, chemically named as polyhydroxylated secondary and tertiary amines and found to be widespread in plants and microorganisms. Thanks to their structural similarity to sugar molecules and excellent metabolic stability, iminosugars are endowed with a high pharmacological potential for a wide range of diseases such as viral infections, tumor metastasis, AIDS, diabetes and lysosomal storage disorders[1–11].

Iminosugars are generally classified into five structural classes: pyrrolidines, piperidines, indolizidines, pyrrolizidines and nortropanes[12]. Hydroxypiperidines are structurally six-membered iminosugars. Some of the hydroxypiperidines such as 1,5-dideoxy-1,5-iminohexitol derivatives have now been commercialized as drugs to treat type II diabetes mellitus, type I Gaucher disease, Niemann-Pick disease type C (NP-C) and Fabry disease[13–18]. Other Hydroxypiperidines like 1,5-Dideoxy-1,5-imino-ribitol and 1,5-Dideoxy-1,5-imino-arabinitol derivatives have also attracted considerable attention as enzyme inhibitors that mimic glycoside and nucleoside substrates. For example, 1,5-dideoxy-1,5-imino-ribitol derivatives was found to be a potent inhibitor of bovine β-galactosidases and almond β-glucosidase[19], while 1,5-Dideoxy-1,5-imino-arabinitol N-carboxypentyl derivatives permitted the isolation of pure α-L-fucosidase from bovine kidney homogenate[20].

There are a diversity of synthetic methodologies have been developed to access iminosugars in hydroxypyrrolidines series[21–25], while the reports for hydroxypiperidine iminosugars synthesis, especial for hydroxypiperidine of pentitols, are limited[26]. Therefore, there is a need to develop a simple method for the preparation of 1,5-Dideoxy-1,5-imino-ribitol and 1,5-Dideoxy-1,5-imino-arabinitol (Fig. 1). In this report, we like to present an efficient and environmentally friendly route for 1,5-dideoxy-1,5-imino-ribitol and 1,5-dideoxy-1,5-imino-L-arabinitol synthesis (Scheme 1) from D-ribose. The synthetic strategy employs many principles of Green Chemistry such as avoiding toxic or noxious chemical, and recycling and reusing the reagents[27].

The oxidation of D-ribose to D-ribonolactone is the critical and also the most difficult reaction in our proposed route. Pd–Bi/C heterogeneous catalyst[28] with molecular oxygen has been successfully applied to directly convert D-ribose to D-ribonolactone. However, Bi–gluconate complexes formed due to the interaction between the leached Bi (from Pd-Bi/C catalyst) and glucose substrate would contaminate the gluconic acid products. As a

Western Digital Company, 5601 Great Oaks Parkway, San Jose, CA 95119-1003, USA. ✉email: fanao2013cn@gmail.com

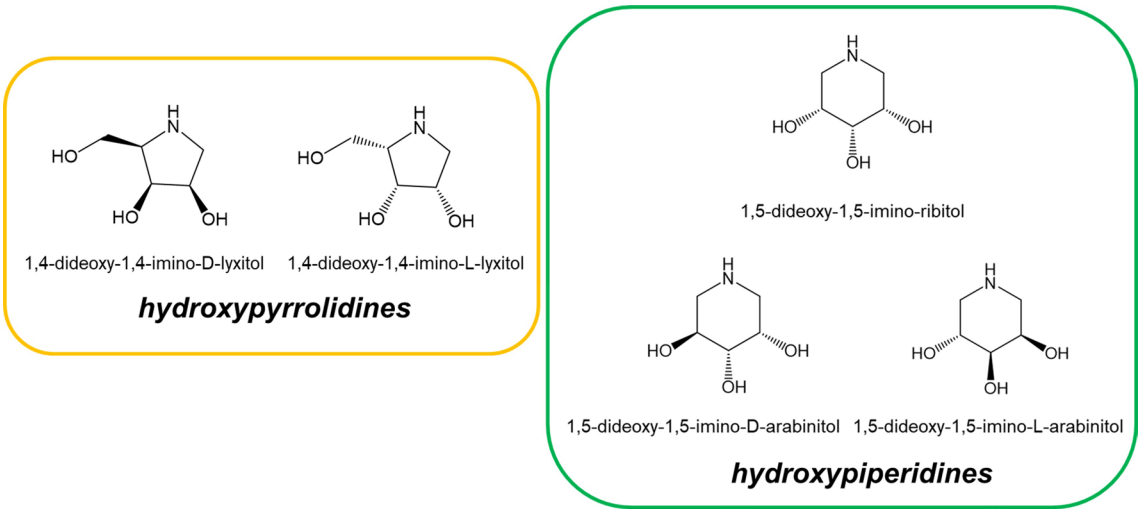

Figure 1. Structures of some hydroxypyrrolidine and hydroxypiperidine iminosugars.

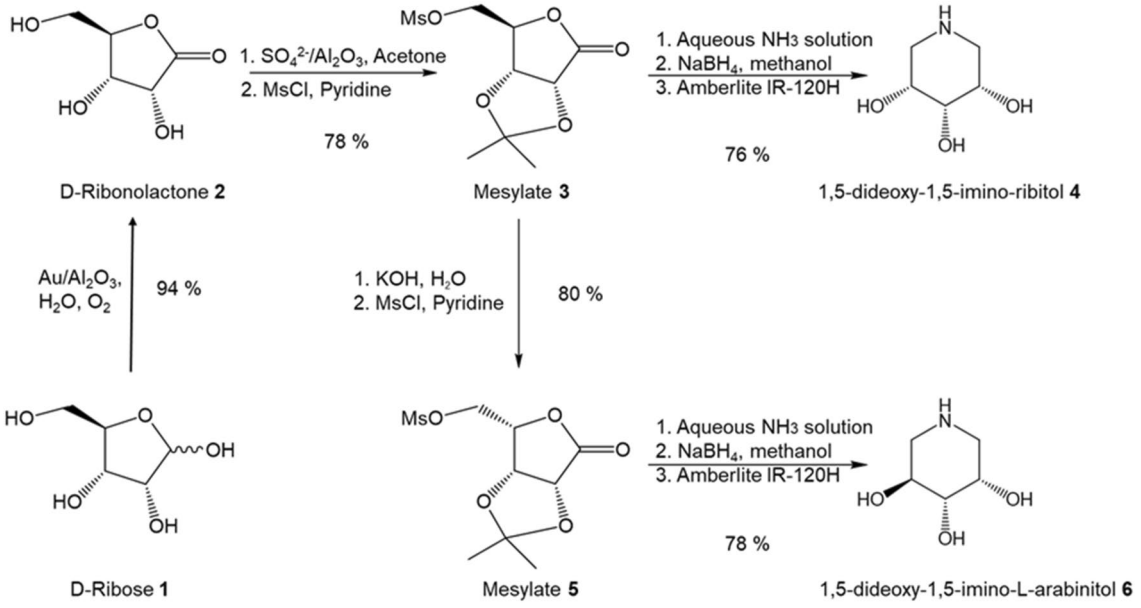

Scheme 1. Synthesis route from D-ribose to 1,5-dideoxy-1,5-imino-D-ribitol 4 and 1,5-dideoxy-1,5-imino-L-arabinitol **6.**

result, further purification of products are needed, introducing large amounts of metal pollution[29]. Additionally, to prevent the catalyst poisoning due to the adsorption of the product during reaction, the reaction medium has to be maintained at pH 9.0 by continual addition of alkaline solution. Thus, the alkaline systems induce plenty of wastes (e.g., inorganic salts). Hence, the alkaline-free direct oxidation of D-ribose over heterogeneous catalysts is an ideal green process to pursue. Recently, Song Guo et al.[30] reported a simple incipient wetness protocol to prepare ultra-small gold clusters on TiO_2 through using anthranilic acid as a stabilizing agent. The resultant Au/TiO_2 catalyst exhibits excellent catalytic activity in the alkaline-free oxidation of glucose. Because of the excellent material physical properties of γ-Al_2O_3 such as high thermal stability, large surface area, and superior mechanistic strength, highly mesoporous γ-Al_2O_3 has been widely used in the chemical industry as catalyst support. Moreover, there are abundant of cation vacancies on γ-Al_2O_3 surface[31]. This unique surface structure of γ-Al_2O_3 helps to stabilize Au clusters and prevent clusters agglomeration on its surface[32]. Thus, we decided to explore ultra-small gold clusters on γ-Al_2O_3 (Au/Al_2O_3) as catalyst for alkaline-free oxidation of D-ribose. To achieve small gold particles (2–3 nm) deposited on Al_2O_3 support, a simple solid grinding method was used in catalyst preparation[33]. The applicability of the Scheme 1 to the synthesis of 1,5-dideoxy-1,5-imino-D-arabinitol **10** starting from D-lyxose was also attempted (Scheme 2).

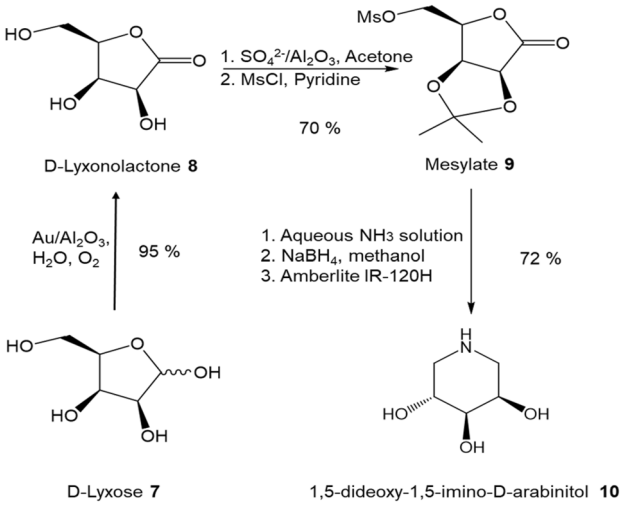

Scheme 2. Synthesis route from D-ribose to 1,5-dideoxy-1,5-imino-D-arabinitol **10.**

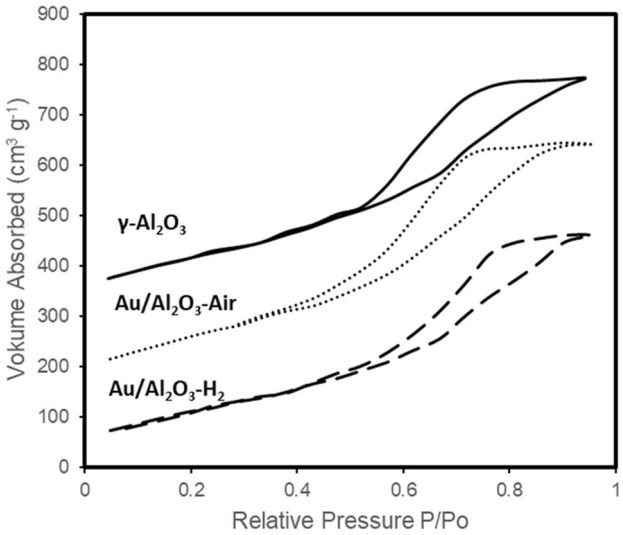

Figure 2. Adsorption/desorption isotherms of γ-Al_2O_3 and Au/Al_2O_3 samples.

Catalyst	Surf. area (m^2 g^{-1})	Pore vol. (m^2 g^{-1})	Ave. pore. diameter (nm)	Au content (wt %)[a]
γ-Al_2O_3	176	0.62	6.14	–
1 wt.% Au/Al_2O_3-Air	161	0.59	5.53	0.93
1 wt.% Au/Al_2O_3-H_2	156	0.58	5.49	0.91

Table 1. Textural properties of γ-Al_2O_3 and γ-Al_2O_3 supported nano Au catalysts. [a]Based on ICP-OES analysis.

Results and discussion

Catalyst characterization. The Au/Al_2O_3 catalysts were prepared through the solid grinding method[33]. The Al_2O_3-supported gold clusters were calcined in static air at 300 °C, and the sample is denoted Au/Al_2O_3-Air. Prior to use, the catalysts were reduced under H_2 flow for 2 h at 150 °C and denoted Au/Al_2O_3-H_2. The nitrogen adsorption–desorption isotherms (Fig. 2) of catalyst samples with type IV shape designated the presence of mesopores with uniform pore size distribution[34]. Table 1 presents the composition, BET surface area, pore volume, average pore diameter of γ-Al_2O_3 support and Au/Al_2O_3 catalysts. The BET surface area, pore volume and

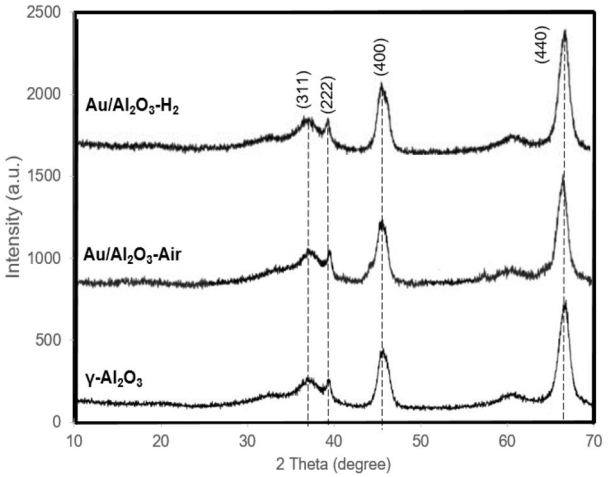

Figure 3. XRD spectra of γ-Al_2O_3 and Au/Al_2O_3 samples.

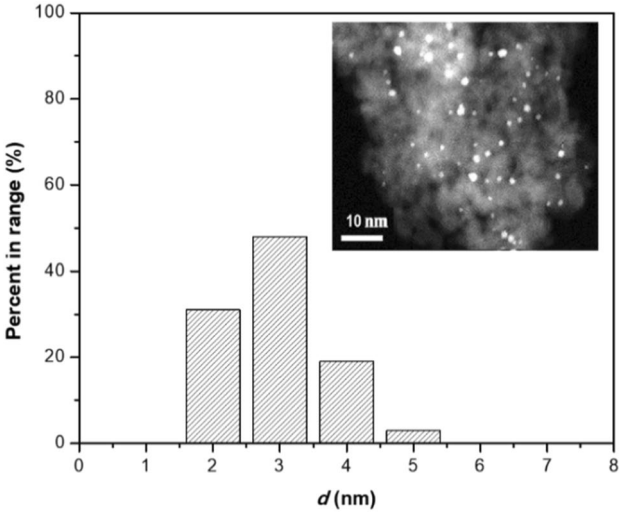

Figure 4. STEM image and size distribution of Au/Al_2O_3-H_2 sample.

average pore diameter were found to be decrease slightly with the loading of Au content, showing that Au was deposited into the pores of γ-Al_2O_3 support.

XRD and TEM were then used on analysing these catalysts to determine the differences in the size and distribution of gold particles on γ-Al_2O_3 support. As shown in Fig. 3, no reflections associated with Au nanoparticles were found on XRD patterns of the Au/Al_2O_3. Actually, the diffraction pattern Au/Al_2O_3 is well in accordance with γ-Al_2O_3 supports (JCPDS 29-63). The XRD results indicate that the gold particles are uniformly dispersed on the oxide surface.

As shown in Fig. 4, the gold nano particles are uniformly distributed on Al_2O_3-H_2 support. The average particle size of an Au/Al_2O_3-H_2 catalyst is 2–3 nm, which was similar to particle size reported in the literature[33]. The small clusters and uniform dispersion results are in agreement with XRD analysis.

To understand the surface state of Au particles on γ-Al_2O_3 surface, the XPS Au 4f spectra were carefully examined for the catalysts before and after H_2 reduction. Based on some XPS spectra obtained from various Au catalysts[35,36] previously, Au $4f_{5/2}$ 87.7 eV and Au $4f_{7/2}$ 84.0 eV could be referred as neutral Au species. As shown in Fig. 5, compared with Au/Al_2O_3 without H_2 reduction, H_2 reduction reduce positive gold species and lead Au 4f peaks shift upward in binding energies (BEs) by 0.3–0.4 eV to neutral Au species. The XPS results reveal that the H_2 reduction could help to reduce positive gold species and produce neutral Au species on the γ-Al_2O_3 surface.

Synthesis of 1,5-dideoxy-1,5-imino-D-ribitol 4 and 1,5-dideoxy-1,5-imino-L-arabinitol 6 from D-ribose. *Oxidation of d-ribose.* In the first step as outlined in Scheme 1, the aerobic D-ribose oxidation was carried out in pure water using O_2 gas (1 MPa) as an oxidant agent. We first examined the catalytic performance of conventional gold nanoparticles (Au/C of 3–5 nm Au particle size) and commercial Pd/C catalyst as well as the synthesized Pd–Bi/C catalyst[28]. It is found that the Au/C catalyst gave a 72% D-ribose conversion with a relatively

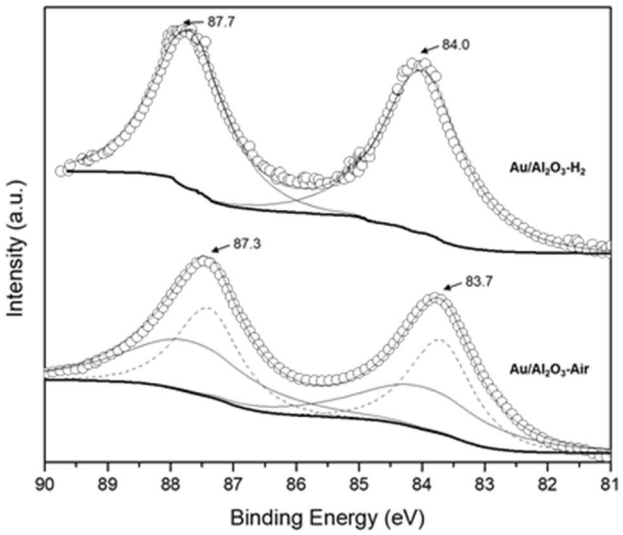

Figure 5. XPS spectra of γ-Al_2O_3 and Au/Al_2O_3 catalysts for Au 4f.

Entry	Catalyst	Temp. (°C)	Conv. (%)	Sel. (%)
1	–	100	–	–
2	1 wt.% Au/C	100	72	82
3	10 wt.% Pd/C	100	45	15
4	10 wt.% Pd-Bi/C	100	36	20
5	1 wt.% Au/Al_2O_3-Air	100	24	> 95
6	1 wt.% Au/Al_2O_3-H_2	100	94	> 95
7	1 wt.% Au/Al_2O_3-H_2	70	67	> 95

Table 2. D-Ribose oxidation under different conditions. Reaction conditions: 0.15 g of D-ribose in 10 mL of H_2O, 36 mg of catalyst, 2 h, 1 MPa O_2. The Au loading of the prepared catalysts is 1 wt.%, and ribose/Au (molar ratio) = 550/1. The conversions (conv.) of ribose and selectivity (Sel.) for ribonolactone were determined by the HPLC analysis.

low ribonolactone selectivity of 82% (Table 2, entry 2). By-products of glutarate and oxalate were formed due to overoxidation and degradation of D-ribose, respectively. The Pd/C and Pd–Bi/C catalysts showed much lower catalytic performance (45% and 36% for D-ribose conversion (Table 2, entries 3 and 4) due to catalyst poison[28]. Intriguingly, their selectivities to ribonolactone was low (≤ 20%)due to the over-oxidized targeted products. For Au/Al_2O_3-Air catalyst, 24% low yield with > 95% selectivity for ribonolactone was obtained. Interesting, simply pretreated the Au/Al_2O_3-Air under H_2 flow for 2 h at 150 °C could significantly improve its catalytic activity, and 93% conversion with > 95% selectivity to ribonolactone (Table 2, entry 6) was achieved. Of note, Au/Al_2O_3 catalyst showed low activity under relatively low reaction temperature conditions (Table 2, entries 7).

Song Guo et al.[30] proposed that the glucose and dioxygen molecules are adsorbed and activated on the Au^0 sites and support, respectively. The occupancy of $Au^{\delta+}$ species at the particles surface by water solvents and oxygen species would block the nearby active Au^0 sites for glucose and O_2 absorption, which would result in a low catalytic performance. From the XPS results (Fig. 5), pretreating the Au/Al_2O_3-Air catalyst under H_2 could almost fully reduce surface $Au^{\delta+}$ species to Au^0 species, which helps to reduce/remove the blocking effect from $Au^{\delta+}$ species and improve the catalytic activity.

The recyclability of Au/Al_2O_3 was evaluated under the same reaction conditions using recycled catalysts. Five cycles were carried out for D-ribose oxidation at 100 °C for 2 h under 1 MPa O_2 using a recycled Au/Al_2O_3 catalyst and fresh reactants. After each reaction, the catalyst was simply recovered by filtration and washed alternately with water and ethanol followed by drying before being used again. The used catalyst was tested in 5 batch reactions without loss of activity and selectivity (Fig. 6). Hence, the results showed that Au/Al_2O_3 is a reusable and selective catalyst for D-ribose oxidation.

Acetalization of d-ribonolactone to 2,3-O-isopropylidene-d-ribonolactone. It was found that anhydrous $CuSO_4$ served as critical Lewis catalyst[28] for the conversion of ribonolactone to 2,3-*O*-isopropylidene-D-ribonolactone. Although relatively high yield (72%) was achieved, the $CuSO_4$ is hard to be fully recovered due to its excellent solubilty in water. Marek Marczewski[37] reported a SO_4^{2-}/Al_2O_3 system, where the acid strength of SO_4^{2-}/Al_2O_3 catalyst could be tuned based on the concentration of H_2SO_4 solution through incipient wetness method. There-

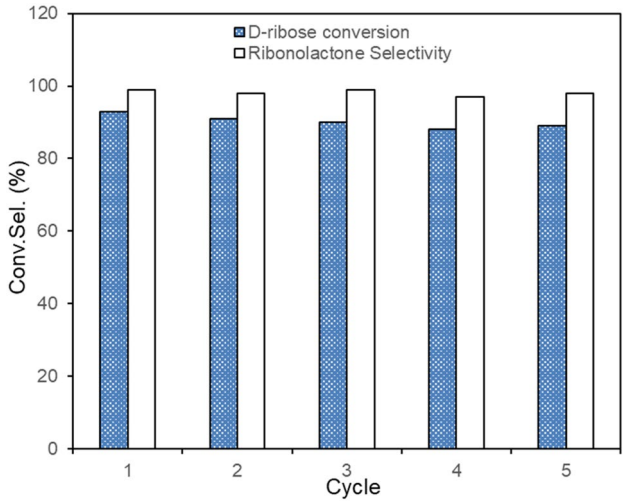

Figure 6. Conversion and selectivity of D-ribose oxidation with recycled Au/Al_2O_3 catalyst.

Entry	Catalyst	Super acid sites (mmol/g)[a)]	Acetone (cm^3)	Condition	Yield 3 (%)
1	–	–	40	Reflux at 60 °C for 6 h	0
2	$CuSO_4$	–	40	Reflux at 60 °C for 2 h	68
3	γ-Al_2O_3	0.082	40	Reflux at 60 °C for 2 h	37
4	1 wt.% SO_4^{2-}/Al_2O_3	0.276	40	Reflux at 60 °C for 2 h	71
5	3 wt.% SO_4^{2-}/Al_2O_3	0.623	40	Reflux at 60 °C for 2 h	86
6	3 wt.% SO_4^{2-}/Al_2O_3		40	Reflux at 60 °C for 4 h	95[b)]
7	9 wt. % SO_4^{2-}/Al_2O_3	1.114	40	Reflux at 60 °C for 2 h	11
8	*Recycled* [c)] 3 wt.% SO_4^{2-}/Al_2O_3	0.448	40	Reflux at 60 °C for 2 h	73
9	*Re-generated* [d)] 3 wt.% SO_4^{2-}/Al_2O_3	0.647	40	Reflux at 60 °C for 2 h	85

Table 3. Acetalization of ribonolactone with acetone.

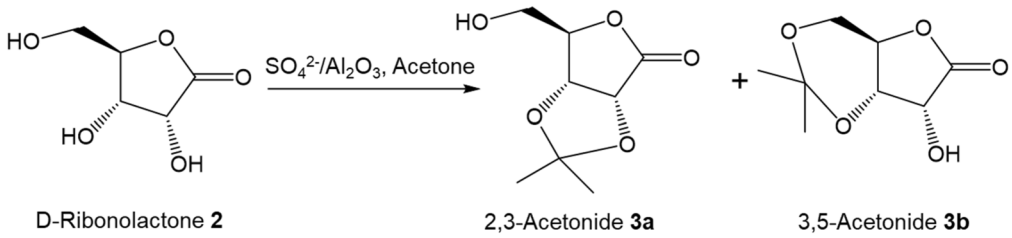

Reaction conditions: 1.5 g of crude D-ribonolactone (10 mmol) in 40 mL of acetone, 3 mmol of catalyst. [a]Were determined by NH_3-TPD analysis. [b]Unknown products probably be 3,4-acetonide[38]. [c]See Recycle procedure in SI. [d]See Re-generation procedure in SI.

fore, we next optimized the condition of SO_4^{2-}/Al_2O_3 catalysts for the acetalization of ribonolactone with acetone to produce 2,3-*O*-isopropylidene-D-ribonolactone.

As shown in Table 3, no 2,3-acetonide **3a** was formed when there was no catalyst in the reaction system. The addition of anhydrous $CuSO_4$ improved the yield to 68% when the reaction mixture was refluxed at 60 °C for 2 h (Table 3, entry 2). Interestingly, the surface sulfates of γ-Al_2O_3 created through H_2SO_4 solution treatment could increase 2,3-acetonide **3a** yield significantly: The yield for commercial γ-Al_2O_3 is only 37%, while the reactions using 1 wt.% SO_4^{2-}/Al_2O_3 and 3 wt.% SO_4^{2-}/Al_2O_3 produced 71% and 85% 2,3-acetonide **3a**, respectively. However, the use of 9 wt.% SO_4^{2-}/Al_2O_3 resulted in charring and only 11% yield of **3a** was obtained (Table 3, entry 7). In addition, extending the refluxing time to 4 h with 3 wt.% SO_4^{2-}/Al_2O_3 catalyst led to the formation of some unknown products (Table 3, entry 6).

To further understand the catalytic performance of the Al_2O_3 samples, catalysts were examined with NH_3-TPD and Pyridine-IR. As shown in Fig. 7, all the catalysts show two NH_3 desorption peaks at around 104 and 524 °C,

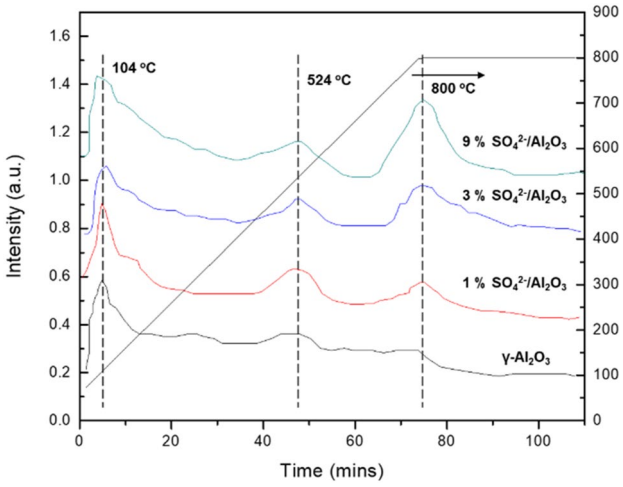

Figure 7. NH_3-TPD curves of Al_2O_3 catalysts.

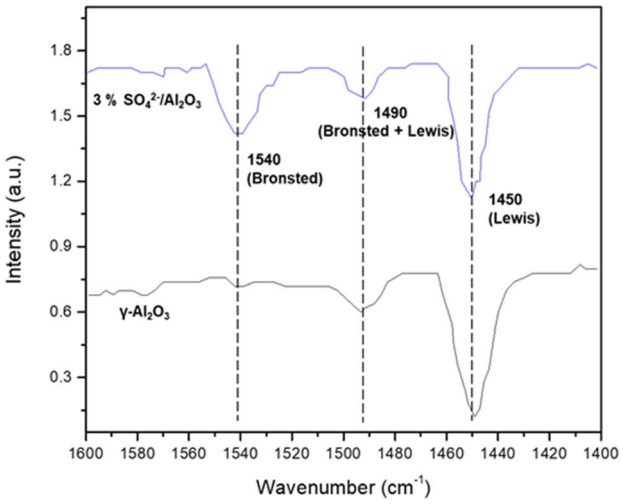

Figure 8. Pyridine-IR spectra of Al_2O_3 catalyst.

which are attributed to the weak and strong acid sites[39–41], respectively. In addition, the third peak at around 800 °C was observed on SO_4^{2-}/Al_2O_3 samples. The NH_3 desorption peak at 800 °C could be ascribed to the super strong acid sites, demonstrating the presence of super-acidic centers on SO_4^{2-}/Al_2O_3 catalysts. The peak at 800 °C was increased with the introduction of more SO_4^{2-} species. Figure 8 shows the Pyridine-IR of the catalysts. Note that both Brønsted and Lewis acid are presence on SO_4^{2-}/Al_2O_3 catalyst, whereas the γ-Al_2O_3 has a very little peak at 1540 cm^{-1}, indicating that there is only a small amount of Brønsted acid sites on γ-Al_2O_3 surface. Thus, the good catalytic activity of the 3 wt.% SO_4^{2-}/Al_2O_3 should be from the synergetic effect of Brønsted and Lewis acid sites as well as its appropriate amount of surface super-acid sites.

It was found that the catalytic acivities of recycled SO_4^{2-}/Al_2O_3 catalysts dropped significantly (Table 3, entry 9) even after re-calcination at 500 °C for 24 h under dry air. The total super acid sites of recycled 3 wt.% SO_4^{2-}/Al_2O_3 sample was reduced to 0.448 mmol/g comparing to 0.623 mmol/g of fresh 3 wt.% SO_4^{2-}/Al_2O_3, indicating the release of substantial sulfate species from Al_2O_3 surface in reaction (Figure S1). To recover the performance of SO_4^{2-}/Al_2O_3 catalyst, re-deposition of SO_4^{2-} on spent catalyst (upto 3 wt.%) by incipient wetness method is required (Table 3, entry 10).

Treated 2,3-acetonide **3a** with methanesulfonyl chloride (MsCl) in pyridine to afford mesylate **3** as yellow crystals (91% yield)[38,42]. Mesylate **3** then was treated with aq ammonia and worked up[44], the 2,3-*O*-isopropylidene ribonolactam could be isolated crystalline in 84% yield. The carbonyl group on the anomeric carbon of the resulting lactam was reduced with $NaBH_4$ in methanol to give colorless syrup (95% yield)[28]. Finally, the resulting syrup was hydrolyzed using acidic Amberlite IR-120H resin to afford 1,5-dideoxy-1,5-imino-D-ribitol **4** in 96% yield. On the other pathway, treated mesylate **3** with potassium hydroxide to inverse the reacting carbon center and then followed by reacting with MsCl in pyridine to afford mesylate **5** in 80% yield[43]. Following the same experiment procedures (treated with aq ammonia, reduction with $NaBH_4$ and hydrolysis using acidic Amberlite

Entry	Reagents	Acetone (cm^3)	Condition	Yield 9 (%)
1	$CuSO_4$	40	Reflux for 4 h	< 5
2	γ-Al_2O_3	40	Reflux for 4 h	0
3	1 wt.% SO_4^{2-}/Al_2O_3	40	Reflux for 4 h	33[a]
4	3 wt.% SO_4^{2-}/Al_2O_3	40	Reflux for 4 h	49[b]
5	3 wt.% SO_4^{2-}/Al_2O_3	40	Stir at RT for 18 h	43
6	9 wt.% SO_4^{2-}/Al_2O_3	40	Reflux at for 4 h	< 5
7	MsOH (15 mmol)	40	Stir at RT for 18 h	27

Table 4. Acetalization of lyxonolactone with acetone.

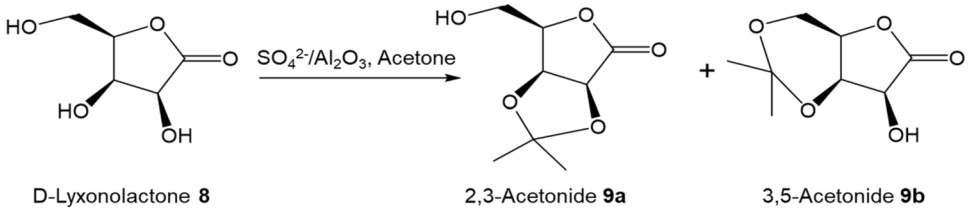

D-Lyxonolactone **8** 2,3-Acetonide **9a** 3,5-Acetonide **9b**

Reaction conditions: 1.5 g of crude D-lyxonolactone (10 mmol) in 40 mL of acetone, 3 mmol of catalyst. Molar ratio of 2,3-acetonide **9a** to 3,5-acetonide **9b**: [a]4:1. [b]3:1.

IR-120H) described above to obtain 1,5-dideoxy-1,5-imino-L-arabinitol **6**. Hence, through above novel and environmental friendly synthetic route, 1,5-dideoxy-1,5-imino-D-ribitol **4** and 1,5-dideoxy-1,5-imino-L-arabinitol **6** was synthesized from D-ribose with an overall yield of 54% and 46%, respectively. The yield for **4** is better than those synthesized from D-ribonolactone (38%) and allylic alcohol (30%)[43]. The yield for **6** is also significantly higher than those from using D-ribose (5–27%)[19]. and L-lyxose (8%)[44] as starting materials. In addition, this synthetic strategy shows more environmental benefit and utilizes more principles of green chemistry than those conventional routes[19,43,44].

The generality of this new synthetic protocol was tested for the synthesis of 1,5-dideoxy-1,5-imino-D-arabinitol **10** from D-lyxose (Scheme 2). D-lyxonolactone could be obtained by oxygenation of the far cheaper D-galactose by the Humphlett oxygenation[45]. However, the yield is low (68%) and potassium D-lyxonate instead of D-lyxonolactone was obtained, which requries extra work to convert potassium D-lyxonate to D-lyxonolactone. Different from Humphlett oxygenation, the aerobic oxidation of D-lyxose **7** with 1 wt.% Au/Al_2O_3 gave higher yield of desirable lactone product and > 99% conversion was achieved after 3 h. The selectivity to D-lyonolactone was > 95%.

Table 4 shows the transformation of D-lyxonolactone **8** to 2,3-*O*-isopropylidene-D-lyxonolactone **9a** under different reaction conditions. The yield for **9a** was < 5% with the use of $CuSO_4$ or γ-Al_2O_3 in reaction (Table 4, entries 1 and 2). When the reaction mixture were refluxed over 1 and 3 wt.% SO_4^{2-}/Al_2O_3, the isomer 3,5-acetonide **9b** was formed. Refluxing the reaction mixture over 9 wt.% SO_4^{2-}/Al_2O_3 charred the reactant and products. To achieve single isomer product acetonide **9a**, the reaction mixture was stirred for 18 h at room temperature, a 43% yield of **9a** could be obtained over 3 wt.% SO_4^{2-}/Al_2O_3, which is significantly improved comparing with 27% yield through using methane sulfonic acid as catalyst. Fortunately, the significant difference in solubility of D-lyxonolatone **8** and 2,3-acetonide **9a** allows them to be easily separated with liquid–liquid (ethyl acetate/water) extraction. In turn, it was possible to recover the unreacted lyxonolatone and carry out further batch reactions to improve the yield. About 80% yield was achieved after three cycles of the reaction. Compound **9a** was next reacted with MsCl in pyridine solution followed by reducing the carbonyl group on the anomeric carbon of the resulting lactam with $NaBH_4$ in methanol, then hydrolyzing over acidic Amberlite IR-120H resin to produce 1,5-dideoxy-1,5-imino-D-arabinitol **10**[46]. The overall yield of 1,5-dideoxy-1,5-imino-D-arabinitol **10** was 48%. The yield to D-arabinitol **10** can be compared with previously reported yields of 40% from D-arabinose[20].

Conclusion

The novel strategy for synthesis of the iminosugars 1,5-dideoxy-1,5-imino-ribitol and 1,5-dideoxy-1,5-imino-DL-arabinitol synthesis was tested out in an environment friendly route starting from naturally occurring D-ribose and D-lyxose. Using ultra small gold clusters on Al_2O_3 (Au/Al_2O_3) could effectively oxidize D-ribose and D-lyxose to corresponding lactones under alkaline-free condition. SO_4^{2-}/Al_2O_3 showed good catalytic activities to replace homogenous Concentrated HCl and MsOH catalysts for acetalization of D-ribonolactone and D-lyxonolactone. The synthetic route resulted in good overall yields of 1,5-dideoxy-1,5-imino-D-ribitol of 54%, 1,5-dideoxy-1,5-imino-D-arabinitol of 48% and 1,5-dideoxy-1,5-imino-L-arabinitol of 46%. In addition, the heterogeneous catalysts and reagents applied in this synthetic strategy show environmental benefit and utilize the principles of green chemistry.

Experimental section

See experiment detail in supplemental information.

Received: 27 March 2021; Accepted: 6 August 2021
Published online: 19 August 2021

References

1. Compain, P. & Martin, O. R. (eds) *Iminosugars: From Synthesis to Therapeutic Applications* (Wiley, 2007).
2. Butters, T. D., Dwek, R. A. & Platt, F. M. Therapeutic applications of imino sugars in lysosomal storage disorders. *Curr. Top. Med. Chem.* **3**(5), 561–574 (2003).
3. Melo, E. B. D., Gomes, A. D. S. & Carvalho, I. α- and β-glucosidase inhibitors: Chemical structure and biological activity. *Tetrahedron* **62**(44), 10277–10302 (2006).
4. Durantel, D., Alotte, C. & Zoulim, F. Glucosidase inhibitors as antiviral agents for hepatitis B and C. *Curr. Opin. Investig. Drugs* **8**(2), 125–129 (2007).
5. Whitby, K., Taylor, D., Patel, D., Ahmed, P. & Tyms, A. S. Action of celgosivir (6 O-butanoyl castanospermine) against the pestivirus BVDV: Implications for the treatment of hepatitis C. *Antiviral Chem. Chemother.* **15**(3), 141–151 (2004).
6. Watson, A. A., Fleet, G. W. J., Asano, N., Molyneux, R. J. & Nash, R. J. Polyhydroxylated alkaloids—Natural occurrence and therapeutic applications. *Phytochemistry* **56**(3), 265–295 (2001).
7. Dwek, R. A., Butters, T. D., Platt, F. M. & Zitzmann, N. Targeting glycosylation as a therapeutic approach. *Nat. Rev. Drug Discov.* **1**(1), 65–75 (2002).
8. Butters, T. D., Dwek, R. A. & Platt, F. M. Molecular analysis of three gain-of-function CHO mutants that add the bisecting GlcNAc to N-glycans. *Glycobiology* **15**(1), 43–53 (2005).
9. Greimel, P., Spreitz, J., Stutz, A. E. & Wrodnigg, T. M. Iminosugars and relatives as antiviral and potential anti-infective agents. *Curr. Top. Med. Chem.* **3**(5), 513–523 (2003).
10. Caines, M. E. C. *et al.* The structural basis of glycosidase inhibition by five-membered iminocyclitols: The clan A glycoside hydrolase endoglycoceramidase as a model system. *Angew. Chem. Int. Ed.* **46**(24), 4474–4476 (2007).
11. Wrodnigg, T. M., Steiner, A. J. & Ueberbacher, B. J. Natural and synthetic iminosugars as carbohydrate processing enzyme inhibitors for cancer therapy. *Anti-Cancer Agents Med. Chem.* **8**(1), 77–85 (2008).
12. Malinowski, M. *et al.* Stereocontrolled synthesis of polyhydroxylated bicyclic azetidines as a new class of iminosugars. *Org. Biomol. Chem.* **16**(25), 4688–4700 (2018).
13. Horne, G., Wilson, F. X., Tinsley, J., Williams, D. H. & Storer, R. Iminosugars past, present and future: Medicines for tomorrow. *Drug Discov. Today* **16**(3–4), 107–118 (2011).
14. Asano, N. Iminosugars: The potential of carbohydrate analogs. In *Carbohydrate Chemistry: State of the Art and Challenges for Drug Development* (ed. Cipolla, L.) 279–301 (Imperial College Press, 2016).
15. Wadood, A. *et al.* Selective glycosidase inhibitors: A patent review (2012–present). *Int. J. Biol. Macromol.* **111**, 82–91 (2018).
16. Stirnemann, J. *et al.* A review of Gaucher disease pathophysiology, clinical presentation and treatments. *Int. J. Mol. Sci.* **18**(2), 441–470 (2017).
17. Lyseng-Williamson, K. A. Miglustat: A review of its use in Niemann–Pick disease type C. *Drugs* **74**(1), 61–74 (2014).
18. McCafferty, E. H. & Scott, L. J. Migalastat: A review in Fabry disease. *Drugs* **79**(5), 543–554 (2019).
19. Front, S., Gallienne, E., Thoenig, J. C., Demotz, S. & Martin, O. R. N-Alkyl-, 1-C-Alkyl-, and 5-C-Alkyl-1,5-dideoxy-1,5-imino-(l)-ribitols as galactosidase inhibitors. *ChemMedChem* **11**(1), 133–141 (2016).
20. Legler, G., Stütz, A. E. & Immich, H. Synthesis of 1,5-dideoxy-1,5-imino-d-arabinitol (5-nor-fuco-1-deoxynojirimycin) and its application for the affinity purification and characterisation of α-fucosidase. *Carbohydr. Res.* **272**(1), 17–30 (1995).
21. La ferla, B., Cipolla, L. & Nicotra, F. General strategies for the synthesis of iminosugars and new approaches towards iminosugar libraries. In *Iminosugars: From Synthesis to Therapeutic Applications* (eds Compain, P. & Martin, O. R.) 25–62 (Wiley, 2007).
22. Compain, P., Chagnault, V. & Martin, O. R. Tactics and strategies for the synthesis of iminosugar C-glycosides: A review. *Tetrahedron Asymmetry* **20**(6–8), 672–711 (2009).
23. Stocker, B. L., Dangerfield, E. M., Win-Mason, A. L., Haslett, G. W. & Timmer, M. S. M. Recent developments in the synthesis of pyrrolidine-containing iminosugars. *Eur. J. Org. Chem.* **9**, 1615–1637 (2010).
24. Hernández, D. & Boto, A. Nucleoside analogues: Synthesis and biological properties of azanucleoside derivatives. *Eur. J. Org. Chem.* **11**, 2201–2220 (2014).
25. Nicolas, C. & Martin, O. R. Glycoside mimics from glycosylamines: Recent progress. *Molecules* **23**(7), 1612–1641 (2018).
26. Wood, A. *et al.* Synthetic pathways to 3,4,5-trihydroxypiperidines from the chiral pool. *Eur. J. Org. Chem.* **48**, 6812–6829 (2018).
27. Fan, A., Chuah, G. K. & Jaenicke, S. A novel and environmental friendly synthetic route for hydroxypyrrolidines using zeolites. *Carbohydr. Res.* **472**, 103–114 (2019).
28. Fan, A., Jaenicke, S. & Chuah, G. K. A heterogeneous Pd–Bi/C catalyst in the synthesis of l-lyxose and l-ribose from naturally occurring d-sugars. *Org. Biomol. Chem.* **9**(22), 7720–7726 (2011).
29. Wenkin, M., Ruiz, P., Delmon, B. & Devillers, M. The role of bismuth as promoter in Pd–Bi catalysts for the selective oxidation of glucose to gluconate. *J. Mol. Catal. A Chem.* **180**(1–2), 141–159 (2002).
30. Guo, S. *et al.* Efficient base-free direct oxidation of glucose to gluconic acid over TiO_2-supported gold clusters. *Nanoscale* **11**(3), 1326–1334 (2019).
31. Tsyganenko, A. A. & Mardilovich, P. P. Structure of alumina surfaces. *J. Chem. Soc. Faraday Trans.* **92**(23), 4843–4852 (1996).
32. Yan, Z., Chinta, S., Mohamed, A. A., Fackler, J. P. & Goodman, D. W. The role of F-centers in catalysis by Au supported on MgO. *J. Am. Chem. Soc.* **127**(6), 1604–1605 (2005).
33. Ishida, T. *et al.* Influence of the support and the size of gold clusters on catalytic activity for glucose oxidation. *Angew. Chem. Int. Ed.* **47**(48), 9265–9268 (2008).
34. He, L., Huang, Y., Wang, A., Liu, Y. & Liu, X. Surface modification of Ni/Al_2O_3 with Pt: Highly efficient catalysts for H_2 generation via selective decomposition of hydrous hydrazine. *J. Catal.* **298**, 1–9 (2013).
35. Haruta, M., Yamada, N., Kobayashi, T. & Iijima, S. Gold catalysts prepared by coprecipitation for low-temperature oxidation of hydrogen and of carbon monoxide. *J. Catal.* **115**(2), 301–309 (1989).
36. Visco, A. M. *et al.* X-ray photoelectron spectroscopy of Au/Fe_2O_3 catalysts. *Phys. Chem. Chem. Phys.* **1**(11), 2869–2873 (1999).
37. Marczewski, M. *et al.* Acidity of sulfated oxides: Al_2O_3, TiO_2 and SiO_2. Application of test reactions. *Phys. Chem. Chem. Phys.* **6**(9), 2513–2522 (2004).
38. Henriette, K., Inge, L. & Christian, P. Synthesis of L-Ribono- and L-Lyxono-lactone. *Acta Chem. Scand.* **48**, 675–678 (1994).
39. Zhao, J., Yue, Y., Hua, W., He, H. & Gao, Z. Catalytic activities and properties of sulfated zirconia supported on mesostructured gamma-Al_2O_3. *Appl. Catal. A-Gen.* **336**(1–2), 133–139 (2008).
40. Chen, W. H., Ko, H. H. & Sakthivel, A. A solid-state NMR, FT-IR and TPD study on acid properties of sulfated and metal-promoted zirconia: Influence of promoter and sulfation treatment. *Catal. Today* **116**(2), 111–120 (2006).
41. Bedia, J., Ruiz-Rosas, R., Rodríguez-Mirasol, J. & Cordero, T. Kinetic study of the decomposition of 2-butanol on carbon-based acid catalyst. *AIChE J.* **56**(6), 1557–1568 (2010).

42. Batra, H. *et al.* A concise, efficient and production-scale synthesis of a protected L-lyxonolactone derivative: An important aldonolactone core. *Org. Process Res. Dev.* **10**, 484–486 (2006).
43. Godskesen, M., Lundt, I., Madsen, R. & Winchester, B. Deoxyiminoalditols from aldonolactones-V. Preparation of the four stereoisomers of 1,5-dideoxy-1,5-iminopentitols. Evaluation of these iminopentitols and three 1,5-dideoxy-1,5-iminoheptitols as glycosidase inhibitors. *Bioorg. Med. Chem.* **4**(11), 1857–1865 (1996).
44. Jaszczyk, J., Li, S., Cocaud, C., Nicolas, C. & Martin, O. R. A practical approach to dideoxy-1,4- and 1,5-iminopentitols from protected sugar hemiacetals. *Carbohydr. Res.* **1**, 107855 (2019).
45. Humphlett, W. J. Synthesis of some esters and lactones of aldonic acids. *Carbohydr. Res.* **4**, 157–164 (1967).
46. Legler, G., Stütz, A. E. & Immich, H. Synthesis of 1,5-dideoxy-1,5-imino-D-arabinitol (5-nor-L-fuco-l-deoxynojirimycin) and its application for the affinity purification and characterisation of a-L-fucosidase. *Carbohydr. Res.* **272**, 17–30 (1995).

Author contributions

H.G. contributed to perform the experiment and write the manuscript. A.F. contributed the conception of the study and manuscript preparation.

Competing interests

The authors declare no competing interests.

Additional information

Supplementary Information The online version contains supplementary material available at https://doi.org/10.1038/s41598-021-96231-9.

Correspondence and requests for materials should be addressed to A.F.

Reprints and permissions information is available at www.nature.com/reprints.

Publisher's note Springer Nature remains neutral with regard to jurisdictional claims in published maps and institutional affiliations.

Open Access This article is licensed under a Creative Commons Attribution 4.0 International License, which permits use, sharing, adaptation, distribution and reproduction in any medium or format, as long as you give appropriate credit to the original author(s) and the source, provide a link to the Creative Commons licence, and indicate if changes were made. The images or other third party material in this article are included in the article's Creative Commons licence, unless indicated otherwise in a credit line to the material. If material is not included in the article's Creative Commons licence and your intended use is not permitted by statutory regulation or exceeds the permitted use, you will need to obtain permission directly from the copyright holder. To view a copy of this licence, visit http://creativecommons.org/licenses/by/4.0/.

© The Author(s) 2021